05

Electroplasticity model for amorphous metal alloys

© E.E. Slyadnikov,[1,2] I.Yu. Turchanovsky[1]

[1] Federal research Center for Information and Computational Technologies,
630090 Novosibirsk, Russia
[2]Tomsk State University of Control Systems and Radioelectronics,
634034 Tomsk, Russia
e-mail: eeslyadnikov@gmail.com

Received October 7, 2024
Revised July 1, 2025
Accepted July 8, 2025

On the basis of the first and second laws of thermodynamics, it was shown that dynamics of the first-order non-equilibrium structural transition from a low-temperature elastic (glassy state) into a high-temperature inelastic state (supercooled liquid state) during electric current pulse propagation was described by the generalized Landau–Khalatnikov equation for a short-range order parameter. This equation describes a structural transformation that, on the one hand, is stimulated by the current pulse energy impact and, on the other hand, takes place in a stress field. The proposed non-equilibrium transition model was used to formulate a physical picture (including causes, conditions and mechanism) of an electroplastic deformation effect in amorphous metal alloys under mechanical load when an electric current pulse is passed, analyze experimental findings, and evaluate physical properties leading to this effect.

Keywords: amorphous metal alloys, electroplastic deformation, mathematical model, electric current pulse, non-equilibrium structural transition.

DOI: 10.61011/TP.2025.10.62093.316-24

Introduction

In [1–4], an electric current pulse (ECP) effect on the behavior of dependences $\sigma(\varepsilon)$ (σ — stress, ε — strain) was experimentally investigated in samples ($80 \times 3.5 \times 0.02$ mm) made from cobalt-base amorphous metal alloys (AMA). Simultaneously with the uniaxial quasistatic tension of samples along the long side (80 mm) in the elasticity region (stress variation range $100\,\text{MPa} < \sigma < 1\,\text{GPa}$, strain rate $\sim 4 \cdot 10^{-5}\,\text{s}^{-1}$), pulses with the current density j in the range from $1 \cdot 10^8$ to $5 \cdot 10^9\,\text{A/m}^2$ were passed. Pulses with the duration $\tau_1 \sim 2.5$ ms and pulse-time ratio ~ 12 s were used. After a series of pulses with j in the range from 10^8 to $10^9\,\text{A/m}^2$, the structure of elastically deformed amorphous alloys remains X-ray amorphous.

In tension of AMA samples with simultaneous transmission of ECP with $4 \cdot 10^9 > j \geq 5 \cdot 10^8\,\text{A/m}^2$, diagrams $\sigma(\varepsilon)$ showed a short-term (less than 1 s) stress relief followed by full restoration of the trend of $\sigma(\varepsilon)$. For example, with initial stress $\sigma \sim 900$ MPa and elastic strain $\varepsilon \sim 0.9\,\%$, a current pulse with $j \sim 4 \cdot 10^9\,\text{A/m}^2$ and $\tau_1 \sim 2.5$ ms induces a short-term increase in room temperature of the sample by 65 K and a stepwise stress relief $\Delta\sigma \sim 400$ MPa is observed, i.e. electroplastic deformation (EPD) [1]. The pulse-induced stress relief is almost 1.5 times larger than the stress relief during slow furnace heating from room temperature to 65 K due to thermal expansion and common thermally-activated processes corresponding to such heating. Due to a low activation energy, short-range atomic order (SRO) homostructural thermal fluctuations are the most probable thermally-activated processes flowing during slow furnace heating to 65 K, however, their concentration is low [1–4]. Therefore, the sample stress relief is caused not only by thermal expansion and common thermally-activated processes, but also by another collective mechanism associated with the ECP-induced structural transformation and inelastic atomic rearrangements (SRO heterostructural thermal fluctuations) [1–4]. Using a synchrotron source, it was (*in situ*) experimentally found [5] that uniaxial tension in nonlinear elastic deformation leads to SRO AMA modification that is expressed in a small anisotropic change of distances (by proportions of percent) between first nearest neighbour atoms.

AMA deformation in the nonlinear elasticity region and moreover in the plasticity region is accompanied by heat propagation and absorption [6–8]. Phenomenological theories of dynamic continuum behavior encompass several methods of considering dissipative effects that go along with deformation. The first method is to introduce viscous stress depending on the strain rate [9]. The second approach states the existence of internal dynamic state variables (order parameters) [10–13] affecting the free system energy. Variation of an internal state variable with time is described by a differential evolution equation where stress occurs. Inelastic strain in AMA may be also described using a theory of non-equilibrium structural transitions (NST) in self-organizing systems (synergetic systems) [14,15].

In [16], a phenomenological description of amorphous plasticity was made on the basis of physical principles

of non-equilibrium thermodynamics and molecular models. Taking into account the correlation between macroscopic deformation processes and sybnanostructural and nanostructural rearrangements, paper [17] formulated a microscopic model of inelastic (pseudoelastic, retarded elastic [13]) deformation in AMA stimulated by external mechanical impact. Physical mechanisms and mathematical models of heat pulse impact of crystallization, nanocrystallization and melting on first-order NST were proposed in [18–20]. Analytical data obtained for first-order NST was verified by means of computational molecular dynamics simulation [21]. Findings in [18–21] qualitatively and quantitatively describe NST patterns in heat-treatment-stimulated AMA.

Classical concept of ECP impact on EPD in metals contains three assumptions [22]. First, direct transmission of conductivity electron force pulses and energy to dislocations (electron wind) is possible. Second, the pulse exerts an electrodynamic effect (so-called pinch and skin-effect). Third, when ECP travels, Joule heat is released and thermal expansion of the sample takes place.

Since there are no dislocations in AMA, the electron wind cannot cause the EPD effect. The level of additional stresses is much lower than the elastic limit due to the pinch and skin effect, and they cannot cause the EPD effect. The EPD effect in AMA cannot be explained either by only thermal expansion of the sample that occurs when the Joule heat is released. Thus, the classical concept of ECP impact on EPD in AMA must be extended.

In contrast to crystals, the amorphous medium has a special (non-crystalline) SRO and excess free volume (EFV), and is subnanostructurally and nanostructurally inhomogeneous [1–8]. There are many SRO clusters and nanoclusters having significant EFV. These SRO clusters and nanoclusters can undergo inelastic atomic rearrangements (SRO and medium-range order heterostructural thermal fluctuations) during external energy pumping and stress application [17].

It is important to develop a model [17] for describing the EPD effect during ECP propagation because heat pulse transmission simultaneously with stress application exerts already a synergistic thermomechanical impact. This work describes a physical picture (including the cause, condition and mechanism) of the EPD effect in AMA during ECP propagation on the basis of knowledge about NST in self-organizing systems [10–21], and evaluates the physical properties causing this effect.

1. Model of the EPD effect during ECP propagation

When the stress exceeds the elasticity limit, then a hysteresis loop occurs at the loading–unloading cycle of curve $\sigma(\varepsilon)$, consequently, heat is released and the sample temperature varies [6,7]. Therefore, on the one hand, thermodynamics shall be used to describe inelastic deformation processes accompanied with temperature variation [23]. In addition, the inelastic deformation process comes with energy dissipation and becomes non-equilibrium, accordingly. Therefore, on the other hand, when using thermodynamics [23], general principles of mechanics shall be maintained, but the second law of non-equilibrium thermodynamics shall be used and, for continua, takes a form of the Clausius–Duhem inequality for the entropy production rate [14–16].

Since the uniaxial quasistatic tension and current transmission take place along the long side (80 mm) of the sample, then a deformed AMA rod model is used to simplify the thermodynamic analysis. The first law of thermodynamics for such system is written as [10,11,16]:

$$\dot{U} = -\sigma\dot{\varepsilon} + \dot{Q}, \tag{1}$$

where $\dot{U}$ is the specific internal energy variation rate, $-\sigma\dot{\varepsilon}$ is the specific work performed on the system per unit time, σ is the internal stress, ε is the total strain, $\dot{Q}$ is the specific Joule heat energy release rate during ECP propagation. In case of sample tension, σ is negative and $\dot{\varepsilon}$ is positive, therefore the internal system energy increases. Then, we postulate that entropy satisfies the conservation law [10,11,16]:

$$\dot{S} - (\dot{Q}/T) = \Sigma. \tag{2}$$

Here, $\dot{Q}/T$ is the entropy increase rate during Joule heat energy release, T is the absolute temperature in energy units, Σ is the entropy production rate within the system, for example, resulting from a non-equilibrium process flow. The second law of thermodynamics states that the entropy production rate is non-negative [14–16]:

$$\Sigma \geq 0. \tag{3}$$

Substituting $\dot{Q}$ from (1) into (2), the following inequality is derived

$$T\dot{S} - \dot{U} - \sigma\dot{\varepsilon} = T\Sigma \geq 0, \tag{4}$$

that can be conveniently rewritten using the free energy $F(T, \varepsilon)$ and dividing the total strain by the elastic and inelastic components [13,16,17]:

$$F(T, \varepsilon_{el}, \eta) = U(S, \varepsilon_{el}, \eta) - TS, \tag{5}$$

$$\varepsilon = \varepsilon_{el} + \varepsilon_{in} = \varepsilon_{el} + \xi\eta, \quad \varepsilon_{in} = \xi\eta, \tag{6}$$

where ε_{el} is the elastic strain, ε_{in} is the inelastic strain [13,16,17] related to the system's internal dynamic state variable η — a dimensionless order parameter, transformation parameter (share of atoms subjected to transformation), ξ is the coefficient of proportionality equal to inelastic saturation strain (because the number of SRO clusters possessing EFV is finite). Total strain represented as a sum of inelastic and elastic components (6) has a physical cause: slow configurational degrees of freedom of the amorphous system are weakly related to fast vibrational degrees of freedom and, consequently, these degrees of freedom may be separated and described by different parameters.

Then, by means of time differentiation $F(T, \varepsilon_{el}, \eta)$, we obtain

$$\dot{F}(F, \varepsilon_{el}, \eta) = (\partial F/\partial T)\dot{T} + (\partial F/\partial \varepsilon_{el})\dot{\varepsilon}_{el} + (\partial F/\partial \varepsilon_{in})\dot{\varepsilon}_{in}. \quad (7)$$

Substituting relation (4) into (5) and using (7), we obtain

$$[(\partial F/\partial T) + S]\dot{T} + [(\partial F/\partial \varepsilon_{el}) + \sigma]\dot{\varepsilon}_{el} + [(\partial F/\partial \eta) + \xi\sigma]\dot{\eta} = -T\Sigma \le 0. \quad (8)$$

Since the derivatives of independent variables with respect to time are not related to each other, expression (8) consists of separate independent inequalities [10,11,16]. After satisfying the first inequality, we get $S = -(\partial F/\partial T)$ that coincides with the traditional thermodynamic relation at equilibrium. The second inequality may be satisfied in the same way, assuming $\sigma = -(\partial F/\partial \varepsilon_{el})$, which is an equilibrium relation between σ and ε_{el}. Inelastic strain is described as NST, therefore inequality (8) may be satisfied by writing dissipative inequality for the order parameter

$$-[(\partial F/\partial \eta) + \xi\sigma]\dot{\eta} \ge 0. \quad (9)$$

Relation (9) is a particular implementation of condition (3) for NST. Inequality (9) is satisfied if a relation in the form of the generalized Landau–Khalatnikov equation is met [10,11,14,16,17]:

$$\dot{\eta} = -\frac{1}{\tau_\eta E_Q^*}\left[\frac{\partial F}{\partial \eta} + \xi\sigma\right] = -\Gamma\left\{\frac{1}{E_Q^*}\left[\frac{\partial F}{\partial \eta} + \xi\sigma\right]\right\} = -\frac{1}{\tau_\eta}\left(\frac{\partial \tilde{F}}{\partial \eta}\right), \quad \tilde{F} = \frac{[F(\eta) + \xi\sigma\eta]}{E_Q^*}, \quad (10)$$

where $\tau_\eta = \tau_\eta(T)$ is the NST relaxation time, E_Q^* is the typical specific energy, $\Gamma = \frac{1}{\tau_\eta(T)}$ is the reverse relaxation time.

Let's consider possible limitations that follow from the fist and second laws of thermodynamics. Relation for the internal energy variation rate during heat release is written as

$$C_V\dot{T} = \dot{Q} + W = \dot{Q} - \left\{\frac{\partial F}{\partial \eta} + \xi\sigma\right\}\dot{\eta},$$

$$W = -\left\{\frac{\partial F}{\partial \eta} + \xi\sigma\right\}\dot{\eta} = \Gamma\left\{\frac{1}{E_Q^*}\left[\frac{\partial F}{\partial \eta} + \xi\sigma\right]^2\right\}, \quad (11)$$

where C_V is the specific heat capacity with constant volume, T is the absolute temperature in kelvins. By definition, the energy dissipation rate W (11) is a sum of the free energy variation rate $-\frac{\partial F}{\partial \eta}\dot{\eta}$ in the non-equilibrium process and the inelastic strain energy rate $-\xi\sigma\dot{\eta} = -\sigma\dot{\varepsilon}_{in} > 0$ (because with the sample in tension $\sigma < 0$). The second law of thermodynamics (Clausius–Duhem inequality) is written as

$$W = -\frac{\partial F}{\partial \eta}\dot{\eta} - \xi\sigma\dot{\eta} \ge 0, \quad (12)$$

i.e. the energy dissipation rate shall be non-negative. Therefore the non-equilibrium process is accompanied by additional heat release and temperature rise.

For simplicity, let's consider the case $\sigma \to 0$, then $0 \le \eta \le 1$. Suppose $F(\eta)$ is a steadily increasing function that has only one minimum at point $\eta_1 = 0$. It follows from the Clausius–Duhem inequality $W > 0$ (12) that the non-equilibrium process can flow only with $\dot{\eta} < 0$, i.e. a non-equilibrium value of the variable decreases with time and tends to a steady-state equilibrium value $\eta_1 = 0$. Thus, the only possible non-equilibrium process in this case is a relaxation of η from the initial non-equilibrium value$\eta(0) > 0$ to the equilibrium value$\eta_1 = 0$. During the relaxation, the free system energy$F(\eta)$ obviously decreases as η decreases, therefore $W > 0$. Suppose $F(\eta)$ is a continuous nonlinear function having a minimum at $\eta_1 = 0$, one maximum at $\eta = \eta_2 < 1$ and another minimum at $\eta_3 = 1$. Within $0 \le \eta < \eta_2$, $F(\eta)$ is increasing, and within $\eta_2 < \eta \le 1$, the function is decreasing. It follows from $W > 0$ (12) that within $0 \le \eta < \eta_2$ the non-equilibrium process may flow only with $\dot{\eta} < 0$, i.e. only the relaxation process can take place. If, resulting from a strong external impact, the value of η gets within $\eta_2 < \eta < 1$, then the non-equilibrium process can flow only with $\dot{\eta} > 0$, i.e. η increases with time and tends to the steady-state value $\eta_3 = 1$. Thus, the only possible non-equilibrium process in this case is a NST process of η from the initial value$\eta(0)$ to the steady-state value$\eta_3 = 1$. During the NST process stimulated by an external impact, $F(\eta)$ obviously decreases as η decreases, therefore $W > 0$.

According to the physical kinetics [24], homostructural fluctuations (for example, density fluctuations) occur in the system, even in thermodynamic equilibrium at room temperature. When a system in glassy state is superheated above room temperature, heterostructural fluctuations occur in the system due to ECP Joule heat release [24]. Growth of a new structure in supercooled liquid state from an old structure in glassy state is possible only with deviation from thermodynamic equilibrium, i.e. the structure in glassy state shall be in non-equilibrium and metastable state, and shall be superheated above the glass transition temperature due to ECP Joule heat release. The new structure occurs in the old metastable structure from an emerging nucleus. Whereby a nucleus smaller than the critical size is instable and disappears, and a nucleus larger than the critical size is stable and grows. According to the principles of statistical physics [12,24], new structure nuclei may emerge and reach their critical size in their instability region using heterostructural thermal fluctuations that bring the system into a higher free energy state.

The minimum work required to bring the system out of equilibrium is equal to the free system energy variation ΔF. Therefore, probability distribution of the heterostructural order parameter fluctuation is equal to [12,24]:

$$d\omega \sim \exp(-\Delta F/kT).$$

For example, with small deviation from equilibrium

$$\Delta F = \frac{1}{2}(\eta - \eta_1)^2\frac{\partial^2 F}{\partial \eta^2}. \quad (13)$$

Then fluctuation probability at a temperature close to the glass transition temperature T_c will be written as

$$\omega = \frac{1}{\sqrt{2\pi}}\sqrt{\left(\frac{\partial^2 F}{\partial\eta^2}/kT_c\right)}\exp\left[\frac{1}{2}(\eta-\eta_1)^2\frac{\partial^2 F}{\partial\eta^2}/kT_c\right]. \quad (14)$$

Mean square order parameter fluctuation is equal to

$$\langle(\Delta\eta)^2\rangle = \int d\eta(\eta-\eta_1)^2\frac{1}{\sqrt{2\pi}}\sqrt{\left(\frac{\partial^2 F}{\partial\eta^2}/kT_c\right)}$$
$$\times\exp\left[-\frac{1}{2}(\eta-\eta_1)^2\frac{\partial^2 F}{\partial\eta^2}/kT_c\right] = kT_c\left[\frac{\partial^2 F}{\partial\eta^2}\right]^{-1}. \quad (15)$$

At the absolute low-temperature structure instability temperature T_2, where

$$\left(\frac{\partial F}{\partial\eta}\right)_{\eta=0} = \eta^2(\eta-1), \quad \left(\frac{\partial^2 F}{\partial\eta^2}\right)_{\eta=0} = 2\eta(\eta-1)+\eta^2 = 0$$

the mean square order parameter fluctuation deviates.

The next analysis stage involves the formulation of $F(\eta)$ for NST. It was found experimentally that after the end of the pulse the inelastic state becomes instable and the system relaxes into the elastic state [1–4]. It is known that the non-equilibrium relaxation of η to the non-equilibrium η_1 in the non-zero σ field is described by the relaxation equation [12,16,17]:

$$\dot\eta = -\frac{1}{\tau_\eta(T)}[\eta-\eta_1] = -\frac{1}{\tau_\eta(T)}\left[\eta+\frac{\xi\sigma}{E_Q^*}\right]. \quad (16)$$

From (10), (16), it follows that the production rate of clusters with field-oriented SRO is proportional to the difference of fieldwise fluctuation probability and counter-fieldwise fluctuation probability and, therefore, with low field $\frac{-\xi\sigma V_\eta}{k_BT} \ll 1$, is proportional to the Boltzmann constant and σ:

$$\frac{1}{\tau_\eta(T)}\eta_1 = \frac{1}{\tau_\eta}\left[\exp\left\{\frac{-(E_\eta+\xi\sigma V_\eta)}{k_BT}\right\}\right.$$
$$\left.-\exp\left\{\frac{-(E_\eta-\xi\sigma V_\eta)}{k_BT}\right\}\right]$$
$$= -\frac{2\xi\sigma V_\eta}{k_BT}\frac{1}{\tau_\eta}\exp\left\{\frac{-(E_\eta+\xi\sigma V_\eta)}{k_BT}\right\}, \quad (17)$$

where $E_\eta+\xi\sigma V_\eta$ is the heterostructural fluctuation activation energy in the SRO cluster with fieldwise inelastic atom rearrangement, k_B is the Boltzmann constant, V_η is the fluctuation activation volume where cooperative rearrangement of a group of atoms takes place to form SRO under the combined action of heat and stress. Experimental findings [1–4] were obtained in the stress variation range $100\,\text{MPa} < \sigma < 1\,\text{GPa}$, i.e. in the elastic behavior region of the sample without current pulse transmission. By evaluating $\frac{-\xi\sigma V_\eta}{k_BT}$ for typical parameters $\xi = 0.3$; glass transition temperature 700 K; $k_BT = 0.06\,\text{eV}$, $V_\eta = (0.2\cdot10^{-9}\,\text{m})^3 = 8\cdot10^{-30}\,\text{m}^3$; for $\sigma = 100\,\text{MPa}$, we get $-\xi\sigma V_\eta = 1.5\cdot10^{-3}\,\text{eV}$, $\frac{-\xi\sigma V_\eta}{k_BT} = 0.025 \ll 1$; for $\sigma = 900\,\text{MPa}$, we get $-\xi\sigma V_\eta = 1.35\cdot10^{-2}\,\text{eV}$, $\frac{-\xi\sigma V_\eta}{k_BT} = 0.225 \ll 1$. Therefore, achievement of the critical Joule energy in the current pulse is a prerequisite for NST flow and occurrence of inelastic strain, and the stress plays a role of a weak orienting field.

Oriented SRO cluster production rate $\frac{1}{\tau_\eta(T)}\eta_1$ contains the activation energy and obeys Arrhenius law. Therefore

$$\frac{1}{\tau_\eta(T)} = \frac{1}{\tau_\eta\exp\{\frac{E_\eta+\xi\sigma V_\eta}{k_BT}\}} = \omega_0\exp\left\{\frac{-(E_\eta+\xi\sigma V_\eta)}{k_BT}\right\}$$

may be interpreted as an attempt (fluctuation) frequency, therefore (11) for the relaxation process may be written as

$$W = -\left[\frac{\partial F}{\partial\eta}+\xi\sigma\right]\dot\eta = \frac{E_Q^*}{\tau_\eta}\left[\eta+\frac{\xi\sigma}{E_Q^*}\right]^2 > 0, \left(\eta+\frac{\xi\sigma}{E_Q^*}\right) > 0. \quad (18)$$

Let's formulate the physical picture of EPD based on an experimental fact [6] that a crystal sample has much lower resistance (therefore, lower Joule heat release) than the same sample in an amorphous state. The reason for this issubnanostuctural and nanostructural inhomogeneity of the amorphous medium. Therefore, due to inelastic scattering of conductivity electrons on structural irregularities, instantaneous Joule energy release will be also inhomogeneous. Consequently, there are subnanosize and nanosize regions where energy higher than average is released and regions where energy lower than average is released. Therefore, in the SRO cluster and nanocluster with EFV where energy higher than average is released instantaneously, a part of the released Joule energy may transform into potential energy of the SRO cluster or nanocluster, i.e. a part of the released Joule energy is accumulated in the atomic subsystem (in the SRO clusters and nanoclusters with EFV), and when the Joule energy is critical, first-order NST from a glassy state into a supercooled liquid state takes place and the latent transformation energy is absorbed. At the same time, AMA structural state varies and inelastic strain occurs. Supercooled liquid state (amorphous state) is a metastable [24], conditionally stable state, to which a local free energy minimum corresponds, and is separated from the globally stable crystalline state by an energy barrier.

Further discussion is based on the kinetic theory of NST [12,16,17,24]. To describe first-order NST from a low-temperature glassy state to a high-temperature supercooled liquid state in the SRO cluster system with EFV when ECP is passed, SRO parameter, η, a dimensionless quantity characterizing the system's structural state is used [17]. Since NST takes place in a stress field, then there is direct relation between the order parameter and inelastic strain, NST is followed by inelastic strain. Elementary volume of the SRO cluster undergoes inelastic rearrangement with the height increasing in the uniaxial strain direction and with the width and length decreasing in perpendicular directions. Therefore, NST from a low-temperature elastic mechanical

state into a high-temperature inelastic mechanical state may be also suggested in the stress field. Physically, η is a ratio (share) of the number of SRO clusters with EFV subjected to disordering and inelastic strain to the number of all SRO clusters with EFV. With $\sigma \to 0$ in the low-temperature elastic state, η tends to zero, and in the high-temperature inelastic state, η tends to unity. It is assumed that the low-temperature elastic state with respect to η is locally stable, i.e. it is separated from the locally stable high-temperature inelastic state by an energy barrier. The low-temperature elastically deformed structure has the absolute instability temperature T_2, and the high-temperature inelastically deformed structure has the absolute instability temperature T_1 with an indifferent structural equilibrium temperature T_c between them, i.e. $T_2 > T_c > T_1$.

When a current pulse is passed, NST from the low-temperature elastic state into the high-temperature inelastic state in the SRO cluster subsystem is described by the generalized Landau–Khalatnikov equation [12,16,17] for η:

$$\frac{d\eta}{dt} = -\frac{1}{\tau_\eta R_Q^*}[(\partial F/\partial\eta) + \xi\sigma]$$

$$= -\frac{1}{\tau_\eta}\Big[\eta(\eta-\eta_2)(\eta-1) + \frac{\xi\sigma}{E_Q^*}\Big],$$

$$\eta_2 = \frac{1}{2}\Big[1 - \frac{T_0 - T_c + E_J C_V^{-1}}{(T_c - T_1)}\Big], \tag{19}$$

$$\tau_\eta = \tau_0 \exp\Big\{\frac{(E_\eta + \sigma\xi V_\eta)}{k_B T}\Big\}, \tag{20}$$

where τ_η is the NST relaxation time related to the thermal fluctuation frequency of first nearest neighbour atoms from the initial SRO (elastically deformed) into a new oriented SRO subjected to inelastic strain, $(1/\tau_0) = \omega_0 \approx 10^{13}$ Hz; E_J is the specific Joule energy released when a current pulse is passed through the SRO cluster subsystem with EFV; E_J is proportional to the squared mean current J^2, mean conductor resistance R and ECP transmission time τ_1, i.e. $E_J \sim J^2 \cdot R \cdot \tau_1$.

Let's evaluate the critical Joule energy E_J^* and absolute instability temperature T_2 of the low-temperature state of the SRO cluster subsystem with EFV with respect to NST. Suppose that the share of EFV-containing SRO clusters is 0.15. Let the instantaneous Joule heat release mainly only in this SRO cluster subsystem with EFV. Since it was found experimentally that the critical mean heating of the sample from room temperature was 65 K, then the instantaneous increase in the temperature of the SRO cluster system with EFV equal to $E_J^* C_V^{-1}$ will be $E_J^* C_V^{-1} = 65/0.15 = 433$ K. Therefore, the instantaneous temperature of the cluster system with EFV will be $T_* = 300 + 433 = 733$ K and is higher than the AMA glass transition temperature. Thus, the SRO cluster subsystem with EFV can undergo structural transition from the low-temperature glassy state into the high-temperature supercooled liquid state by means of oriented-SRO cluster condensate formation.

Let's consider the behavior of steady states (roots of equations) of a system whose dynamics is described by equation (19). Nonlinear function on the right-hand side of equation (19) with $\sigma \to 0$ and $(T_c - T_1) = (T_2 - T_c)$ has three roots

$$\eta_1 \to 0,\ \eta_2 \to \frac{1}{2}\Big[1 - \frac{T_0 - T_c + E_J C_V^{-1}}{(T_c - T_1)}\Big],\ \eta_3 \to 1,$$

where T_0 is the initial sample temperature. with $T_0 = T_1$ and without a pulse, $E_J = 0$ and $\eta_2 \to 1$, therefore the low-temperature elastic state $\eta_1 \to 0$ is stable, and the high-temperature inelastic state $\eta_3 \to 1$ is absolutely instable. Current pulse energy impact E_J shifts the root

$$\eta_2 \to \frac{1}{2}\Big[1 - \frac{T_0 - T_c + E_J C_V^{-1}}{(T_c - T_1)}\Big]$$

towards the root $\eta_1 \to 0$. With low current pulse energy

$$-\frac{T_0 - T_c + E_J C_V^{-1}}{(T_c - T_1)} \le 1,$$

the low-temperature elastic state of the medium is globally stable, and the high-temperature inelastic state of the medium is locally stable. With high E_J^c, $\eta_2 \simeq \frac{1}{2}$, and the low-temperature elastic and high-temperature inelastic states of the medium are locally instable and are at the indifferent equilibrium point.

$$\frac{T_0 - T_c + E_J^c C_V^{-1}}{(T_c - T_1)} = 0,\ E_J^c C_V^{-1} = T_c - T_0.$$

With critical E_J^* and when the absolute instability temperature of the low-temperature elastic state $E_J^* C_V^{-1} = T_2 - T_0$ has been reached, $\eta_2 = 0$ the low-temperature elastic state of the medium becomes absolutely instable, and the high-temperature inelastic state of the medium is globally stable. If the energy E_J released during ECP transmission reaches E_J^*, and the current pulse impact time exceeds the NST relaxation time τ_η, the energy barrier separating the elastic and inelastic state disappears and the medium fully goes into the inelastic state. Numerical solutions to equation (19) for the initial order parameter fluctuation $\eta(0) = 0.1$ and various current pulse energies $E j \cdot C_V^{-1} = T_1 - T_0$ and $E_j \cdot C_V^{-1} = T_2 - T_0$ are shown in Figure 1.

Uniaxial load applied to an AMA rod almost immediately induces the elastic strain $\varepsilon_1(t)$, that is related to the external stress $f(t)$ via Hooke's law [23]:

$$\varepsilon_1(t) = (1/\mu) f(t),\quad \frac{d\varepsilon_1(t)}{dt} = (1/\mu)\,\frac{df(t)}{dt}. \tag{21}$$

When current pulse is applied, NST described by $\eta(t)$ takes place in the sample and inelastic strain occurs. $\varepsilon_2(t)$ [13,16,17]:

$$\varepsilon_2(t) = \xi\eta(t),\quad \frac{d\varepsilon_2(t)}{dt} = \varepsilon\,\frac{d\eta(t)}{dt}. \tag{22}$$

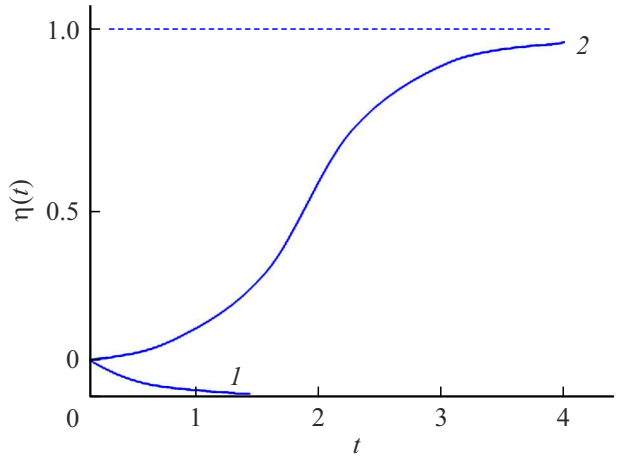

Figure 1. Dependence of the order parameter on time (in terms of relaxation time) for $\eta(0) = 0.1$ and various current pulse energies: *1* — $Ej \cdot C_V^{-1} = T_1 - T_0$, *2* — $Ej \cdot C_V^{-1} = T_2 - T_0$.

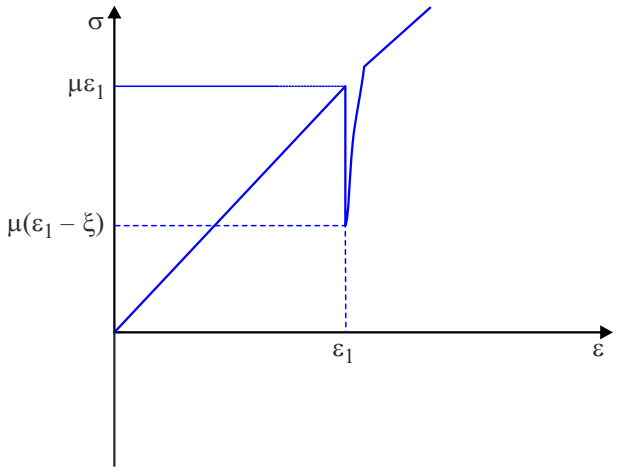

Figure 2. Stress–strain dependence during current pulse transmission.

Total strain ε of the sample may be represented in the form of a sum of elastic and inelastic strains [16,17]:

$$\varepsilon = \varepsilon_1 + \varepsilon_2, \quad \frac{d\varepsilon(t)}{dt} = \frac{1}{\mu}\frac{df(t)}{dt} + \xi\frac{d\eta(t)}{dt}. \tag{23}$$

In the fixed total strain condition ($\varepsilon = \text{const}$, $\dot{\varepsilon} = 0$), equation (23) is reduced to

$$\frac{1}{\mu}\frac{df}{dt} = -\xi\frac{d\eta(t)}{dt}, \quad f = f(\eta), \quad f(0) = \mu\varepsilon_1, \quad \frac{df}{d\eta} = -\xi\mu,$$

$$f(\eta) = f(0) - \xi\mu\eta = \mu(\varepsilon_1 - \xi\eta), \tag{24}$$

$$f(1) = \mu(\varepsilon_1 - \xi). \tag{25}$$

From (24), (25), it can be seen that, without a current pulse and structural transformation ($\eta = 0$), the stress increases proportionally to the strain in the region $0 < \varepsilon < \varepsilon_1$ (Figure 2). When a current pulse is passed, NST ($\eta = 1$) takes place at point ε_1, and inelastic strain $\varepsilon_2(\eta = 1) = \xi$ occurs. Since the total strain is fixed, inelastic strain leads to a decrease in the elastic strain and, consequently, the stress is relieved by $-\xi\mu$ (Figure 2).

After the end of the pulse, the high-temperature inelastic state becomes instable and relaxes into the stable low-temperature elastic state according to the relaxation equation [11,16,17]:

$$\frac{d\eta}{dt} = -\alpha\eta, \quad \frac{d\eta}{\eta} = -\alpha dt, \quad \eta(t) = \exp(-\alpha t),$$

$$\sigma(\eta(t)) = \mu[\varepsilon_1 - \xi\exp(-\alpha t)], \tag{26}$$

where α is the reverse structural stress relaxation time. $\xi\eta(t)$ relaxes exponentially to zero, while the stress grows and relaxes to a value (Figure 2).

2. Summarizing and discussing findings, evaluations and conclusion

On the basis of the first and second laws of thermodynamics, it was shown that dynamics of the first-order non-equilibrium structural transition from a low-temperature elastic (glassy state) into a high-temperature inelastic state (supercooled liquid state) during electric current pulse propagation was described by the generalized Landau–Khalatnikov equation for SRO η. This equation describes NST that, on the one hand, is stimulated by the current pulse energy impact E_J and, on the other hand, takes place in the stress field σ. Since ξ and $(\xi\sigma/E_Q^*)$ are much lower than unity, a weak stress σ only serves to identify a particular orientation of the new SRO.

The proposed NST model was used to formulate a physical EPD picture in AMA exposed to stress when ECP is passed, analyze experimental data [1–4], and evaluate the effect of physical properties.

Physical causes of EPD in AMA are subnanostructural and nanostructural inhomogeneity of the amorphous medium, and a pulse nature of the energy source that allow a part of ECP energy to be accumulated in the form of additional potential energy of SRO atomic clusters and nanoclusters with EFV, and the structural state of the medium changes at the same time. Therefore, due to spatial inhomogeneity of AMA, pulse energy is released inhomogeneously over the medium volume. Due to a pulse nature of the energy source, when ECP is acting, the temperature fails to be balanced over the sample volume and a temperature gradient field occurs. Actually, the pulse energy is released during $\tau_1 = 2.5\,\text{ms}$, and the time of temperature relaxation over the amorphous sample thickness (with dimensions $80 \times 3.5 \times 0.02\,\text{mm}$) l is $\tau_T = (l^2/a) \approx 1\,\text{s}$, $l \approx 10^{-3}\,\text{m}$, $a \approx 10^{-6}\,\text{m}^2/\text{s}$, therefore $\tau_T \gg \tau_1$ is satisfied.

Consequently, when the pulse is acting, energy distribution over the amorphous sample volume becomes even more inhomogeneous and non-equilibrium than before the pulse impact. Therefore, sample regions (atom clusters with EFV, increased potential energy), where high amount of Joule energy was released, undergo non-equilibrium transformation, inelastic strain, etc. NST forced by the inhomogeneous and non-equilibrium energy distribution in AMA when ECP is passed, occurs only in an energy-enriched part of the sample and covers only a part of all atoms. Physical mechanism of NST is the condensation of heterostructural thermal fluctuations of SRO atoms that is enhanced by the combined action of heat and stress. When the pulse energy is low, concentration of clusters subjected to transition into the oriented SRO state is low. When the pulse energy increases, the concentration of oriented SRO clusters increases (and the distance between clusters decreases), and with critical pulse energy, the concentration of oriented SRO clusters becomes such that correlation of order parameter fluctuations occurs, i.e. a fluctuation correlation radius is reached where the probability of simultaneous occurrence of a fluctuation pair is higher that the product of probabilities of two independent fluctuations. At the same time, a sudden increase in the concentration of heterostructural thermal fluctuations of SRO atoms (condensation, condensate formation) is taking place. Since T_2 is the absolute instability temperature of the low-temperature structure, then, with instantaneous heating up to T_2, the cluster subsystem with EFV receives latent first-order NST energy.

When the sample is heated slowly (in a quasi-equilibrium manner) in a furnace to a temperature exceeding the initial temperature by 65 K [1–4], the heat energy is distributed evenly over the volume (there is no temperature gradient field) and this mean specific energy is insufficient any longer for first-order NST in the SRO cluster subsystem with EFV, therefore no inelastic strain occurs.

Achievement of the critical current pulse energy and application of a weak orienting stress are the conditions for implementing EPD in AMA. Physical mechanism of EPD (when the critical value $j \sim 4 \cdot 10^9$ A/m^2 is reached) is a first-order NST process with occurrence of a new oriented SRO of atoms. This structural transition from the low-temperature elastic state to the high-temperature inelastic state is non-equilibrium because energy supplied from external environment (pulse energy release) is necessary for the transition to take place and for the stable inelastic state to exist.

When ECP with $\tau_1 \sim 2.5$ ms and $j \sim 5 \cdot 10^8$ A/m^2 is passed through the AMA sample, a mean energy per atom $w_a \sim 0.8 \cdot 10^{-4}$ eV is released and the mean sample temperature increases by 10 K [1–4]. Moreover, in the elastic strain region, for example, $\varepsilon \sim 10^{-3}$, elastic energy variation per atom is $\sim 10^{-6}$ eV, which is much smaller than the released Joule heat energy. At low ECP energy, a small share of SRO clusters with EFV undergoes inelastic atomic rearrangements oriented in a low stress direction, no NST takes place, therefore a relative stress relief (less the stress relief due to thermal expansion and common thermally-activated processes) is small [1–4].

When the critical current density $j \sim 4 \cdot 10^9$ A/m^2 (released mean energy per atom $w_a \sim 0.52 \cdot 10^{-3}$ eV, mean sample superheating by 65 K) is reached, the SRO cluster (nanocluster) subsystem with EFV becomes instable with respect to the first-order NST followed by occurrence of a new SRO characterized by atom disorder and oriented in the stress direction, i.e. by inelastic strain [17]. NST flows in the subnanocluster subsystem, therefore a relative stress relief (less the stress relief induced by thermal expansion and common thermally-activated processes) is big. When the pulse impact ends,the high-temperature inelastic state becomes instable and the subsystem fully relaxes into the stable low-temperature elastic state (glassy state), therefore the initial trend of curve $\sigma(\varepsilon)$ is restored [1–4].

When the current density increases to $j = 5 \cdot 10^9$ A/m^2 (released mean energy per atom $w_a \sim 0.64 \cdot 10^{-3}$ eV, mean sample superheating by 80 K), the nanocluster subsystem with EFV becomes instable with respect to the first-order NST followed by occurrence of a new medium-range order characterized by high atom disorder (supercooled liquid state) and oriented in the stress direction, i.e. by inelastic strain [17]. NST flows in the nanocluster subsystem, therefore a relative stress relief (less the stress relief induced by thermal expansion and common thermally-activated processes) is much bigger After ECP transmission, the system relaxes quickly only in a part of atom short-range order, the medium-range order atom relaxation time may be much higher than the experiment time. Therefore a part of inelastic strain remains, and the initial trend of curve $\sigma(\varepsilon)$ is restored only partially [1–4]. When the current density becomes even higher, AMA nanocrystallization will start [19] and may be followed by nanostructural shear strain that may be referred to as the plastic strain.

Using experimental data for cobalt-based AMA [1–4] (initial stress $f \sim 900$ MPa, elastic strain $\varepsilon \sim 0.9\,\%$, current pulse with $j \sim 4 \cdot 10^9$ A/m^2 and $\tau_1 \sim 2.5$ ms causes the stress relief $\Delta f \sim 400$ MPa), modulus of elasticity $\mu \sim 100$ GPa, thermal expansion strain $\sim 0.66 \cdot 10^{-2}$ and inelastic saturation strain $\xi \sim 0.34 \cdot 10^{-2}$ may be evaluated from equation (25). Equation (26) and the experimental data [1–4] (after the end of the pulse, the stress relief is restored during ~ 20 s) may be used to evaluate the structural stress relaxation time $\alpha^{-1} \sim 8$ s. Equations (19), (20) and the experimental data [1–4] (pulse duration $\tau_1 \sim 2.5$ ms) may be used to evaluate the NST relaxation time $\tau_\eta < \tau_1 \sim 2.5$ ms.

Thus, the formulated physical picture (including the cause, condition and mechanism) of the EPD effect during ECP transmission qualitatively describes the experimental data [1–4].

Conflict of interest

The authors declare no conflict of interest.

References

[1] S.A. Sidorov, V.A. Fedorov, T.N. Pluzhnikova and others. Vestnik Tambovskogo gos.un-ta. Seriya: estestvennye i tekhnicheskie nauki, **17** (1), 135 (2012) (in Russian).
[2] V.A. Fedorov, T.N. Pluzhnikova, S.A. Sidorov. Izvestiya vuz. Chernaya metallurgiya, **12**, 62 (2013) (in Russian).
[3] V.A. Feodorov, T.N. Plushnikova, S.A. Sidorov, A.V. Yakovlev. Mater. Phys. Mechanics, **20** (1), 67 (2014).
[4] D.Yu. Fedorov, S.A. Sidorov, V.A. Fedorov, T.N. Pluzhnikova, A.V. Yakovlev. Izvestiya vuz. Chernaya metallurgiya, **60**, 7 (538) (in Russian).
[5] M. Stoica, J. Das, J. Bednarcik, H. Franz, N. Mattern, W.H. Wang, J. Eckert. J. Appl. Phys., **104**, 013522 (2008).
[6] K. Sudzuki, K. Khudzimori, K. Khasimoto. *Amorfnye Metally* (Metallurgiya, M., 1987), 328 p. (in Russian).
[7] A.M. Glezer, N.A. Shurygina. *Amorfno-nanokristallicheskiye splavy* (Fizmatlit, M., 2013), 452 p. (in Russian).
[8] G.E. Abrosimova. UFN, **181** (12), 1265 (2011) (in Russian).
[9] L. D. Landau, E. M. Lifshitz. *Teoreticheskaya fizika v 10 tomakh. T. 6 Gidrodinamika* (Fizmatlit, M., 2001) (in Russian)
[10] B.D. Coleman, M.E. Gurtin. J. Chem. Phys., **47**, 597 (1967).
[11] J.R. Rice. J. Mech. Phys. Solids, **19**, 433 (1971).
[12] L.D. Landau, E.M. Lifshitz. *Statisticheskaya fizika* (Nauka, M., 1976) ch. I, (t. V), 584 s. (in Russian).
[13] G.A. Malygin. UFN, **171** (2), 187 (2001) (in Russian).
[14] H Haken. Sinergetika (Mir, M., 1980), 406 s. (in Russian).
[15] I. Prigozhin. R. Defay. *Khimicheskaya termodinamika* (Nauka, Novosibirsk, 1966), 510 s. (in Russian)
[16] Bouchbinder Eran, J.S. Langer. Phys. Rev. E, **80**, 031131 (2009).
[17] E.E. Slyadnikov, I.Yu. Turchanovskiy. ZhTF **93**, 1 (104) (in Russian). (2023). DOI: 10.21883/JTF.2023.01.54069.114-22
[18] E.E. Slyadnikov, Yu.A. Hon, P.P. Kaminsky, I.Yu. Turchanovsky. ZhTF, **88** (3), 374 (2018) (in Russian). DOI: 10.21883/JTF.2018.03.45593.2347
[19] E.E. Slyadnikov, I.Yu. Turchanovskiy. ZhTF **90**, 7 (1136) (in Russian). (2020). DOI: 10.21883/JTF.2020.07.49448.299-19
[20] E.E. Slyadnikov, Yu.A. Hon, P.P. Kaminsky, I.Yu. Turchanovsky. IFZh, **93** (2), 403 (2020) (in Russian).
[21] S.Yu. Korostelev, E.E. Slyadnikov, I.Yu. Turchanovskiy. Izvestiya vuzov. Fizika, **65** (8), 49 (2022) (in Russian).
[22] O.A. Troitsky. Chernaya metallurgiya, **60**, 7 (538) (in Russian). Byulleten nauchno-tekhnicheskoy informatsii, **9**, 65 (2018).(in Russian)
[23] L.D. Landau, E.M. Lifshitz. *Teoriya uprugosti* (Nauka, M., 1987), 247 p. (in Russian).
[24] Y.I. Frenkel. *Kineticheskaya teoriya zhidkostey* (Nauka LO, L., 1975) (in Russian).

Translated by E.Ilinskaya